

# CARMA1 is a critical lipid raft-associated regulator of TCR-induced NF- $\kappa$ B activation

Olivier Gaide<sup>1,\*</sup>, Benoît Favier<sup>2,\*</sup>, Daniel F. Legler<sup>1</sup>, David Bonnet<sup>1</sup>, Brian Brissoni<sup>1</sup>, Salvatore Valitutti<sup>2</sup>, Claude Bron<sup>1</sup>, Jürg Tschopp<sup>1</sup> and Margot Thome<sup>1</sup>

**CARMA1 is a lymphocyte-specific member of the membrane-associated guanylate kinase (MAGUK) family of scaffolding proteins, which coordinate signaling pathways emanating from the plasma membrane. CARMA1 interacts with Bcl10 via its caspase-recruitment domain (CARD). Here we investigated the role of CARMA1 in T cell activation and found that T cell receptor (TCR) stimulation induced a physical association of CARMA1 with the TCR and Bcl10. We found that CARMA1 was constitutively associated with lipid rafts, whereas cytoplasmic Bcl10 translocated into lipid rafts upon TCR engagement. A CARMA1 mutant, defective for Bcl10 binding, had a dominant-negative (DN) effect on TCR-induced NF- $\kappa$ B activation and IL-2 production and on the c-Jun NH<sub>2</sub>-terminal kinase (Jnk) pathway when the TCR was coengaged with CD28. Together, our data show that CARMA1 is a critical lipid raft-associated regulator of TCR-induced NF- $\kappa$ B activation and CD28 costimulation-dependent Jnk activation.**

Engagement of the T cell receptor (TCR) by peptide-major histocompatibility complex (MHC) leads to the activation, proliferation and differentiation of mature T cells. One of the earliest events after TCR triggering is activation of the TCR-proximal Src and Syk family tyrosine kinases, which subsequently initiate the phosphorylation and/or recruitment of specific cellular target proteins, including adaptor molecules, lipases, lipid kinases and Ser-Thr kinases<sup>1</sup>. In combination with signaling cascades initiated from costimulatory receptors, this leads to the formation of membrane-proximal signaling complexes that ultimately induce the activation of transcription factors, including NF- $\kappa$ B, NFAT and AP-1<sup>2,3</sup>.

Several studies have demonstrated a critical role for membrane microdomains, also referred to as lipid rafts, in signal transduction by the TCR<sup>4</sup>. Lipid rafts are characterized by their insolubility in cold non-ionic detergents and have a special lipid composition enriched in cholesterol and glycosphingolipids. Some of the TCR signal transducers—such as Src kinases, linker for activation of T cells (LAT) and Ras—are constitutively associated with lipid rafts<sup>4,6</sup>, whereas others—including CD3 $\zeta$ , ZAP-70, Vav, phospholipase C- $\gamma$ 1 (PLC- $\gamma$ 1), protein kinase C- $\theta$  (PKC- $\theta$ ) and I $\kappa$ B kinase (IKK) components—partition into lipid rafts as a consequence of TCR triggering<sup>7–10</sup>.

Signals that lead to NF- $\kappa$ B activation are essential for T cell activation, but the components of the signaling pathway are still poorly defined<sup>11</sup>. PKC- $\theta$  is a critical component because mice deficient for PKC- $\theta$  show impaired activation of NF- $\kappa$ B<sup>12</sup>. A number of studies have also revealed a critical role for the Bcl10 protein in the NF- $\kappa$ B signaling

pathway in lymphocytes. Bcl10-deficient mice display a lack of NF- $\kappa$ B-dependent T cell activation similar to that observed in PKC- $\theta$ -deficient mice<sup>12,13</sup>; this suggests that Bcl10 and PKC- $\theta$  act along the same TCR-triggered NF- $\kappa$ B pathway.

Bcl10 was originally identified from the t(1;14)(p22;q32) chromosomal translocation associated with an aggressive form of lymphomas of the mucosa associated lymphoid tissue (MALT)<sup>14,15</sup>. It has been suggested that up-regulated expression of wild-type or mutated forms of Bcl10 may promote antigen-independent growth and lymphoma progression through constitutive NF- $\kappa$ B activation<sup>13</sup>. Bcl10 has an NH<sub>2</sub>-terminal caspase recruitment domain (CARD) that mediates both self-oligomerization and binding to the CARD motif of a subfamily of membrane-associated guanylate kinase (MAGUK) proteins called CARD-MAGUKs (CARMAs)<sup>16</sup>, Bcl10-interacting MAGUK proteins (Bimps)<sup>17</sup> or CARD10, CARD11 and CARD14<sup>18,19</sup>.

MAGUKs are scaffolding proteins that bind directly to the cytoplasmic termini of transmembrane proteins and to other signal transduction proteins, thereby organizing specific signaling pathways emanating from plasma membrane receptors at the sites of cell junctions<sup>20,21</sup>. All members of the MAGUK family share a similar COOH-terminal array of protein-protein interaction domains: one to three PDZ domains that generally bind to the cytoplasmic portion of cellular receptors<sup>22</sup> and an SH3 domain that potentially binds proline-rich target sequences<sup>23</sup>, followed by a linker region and a GUK domain, which most likely serves as a protein-protein interaction motif rather than as an active kinase<sup>21</sup>. Upon overexpression, CARMA1 (also known as CARD11 and Bimp3),

<sup>1</sup>Institute of Biochemistry, University of Lausanne, BIL Biomedical Research Center, Chemin des Boveresses 155, CH-1066 Epalinges, Switzerland. <sup>2</sup>INSERM U563, Institut Claude de Prével, CHU Purpan, F-31059 Toulouse, France. \*These authors contributed equally to this work. Correspondence should be addressed to M.T. (Margot.ThomeMiazza@ib.unil.ch).

CARMA2 (also known as CARD14 and Bimp2) and CARMA3 (also known as CARD10 and Bimp1) bind to Bcl10 *via* a CARD-dependent interaction, thereby activating the NF- $\kappa$ B pathway<sup>16–19</sup>. The viral ortholog of Bcl10, vE10, associates with the plasma membrane due to a COOH-terminal lipid modification, and efficient NF- $\kappa$ B activation by vE10 is paralleled by a CARD-dependent membrane translocation of Bcl10<sup>24</sup>. Thus, it is likely that the CARMAs act as membrane-proximal scaffolding proteins that organize Bcl10 and other signaling proteins in the NF- $\kappa$ B-activating pathway emerging from the TCR<sup>16</sup>.

We show here that CARMA1 is a lipid raft-associated protein that binds to the TCR complex and to Bcl10 in an activation-dependent manner. We also demonstrate a critical role for CARMA1 in TCR-induced NF- $\kappa$ B activation and CD28 costimulation-dependent Jnk activation.

## Results

### CARMA1 and Bcl10 recruitment to the TCR

To study the molecular function of CARMA1 in T lymphocytes, we raised a polyclonal antibody (AL220) against a glutathione-S-transferase (GST) fusion protein comprising the NH<sub>2</sub>-terminal CARD motif of

CARMA1. This antibody specifically recognized a band of ~130 kD in a cell extract of 293T cells transfected with vesicular stomatitis virus (VSV)-tagged full-length CARMA1 (**Fig. 1a**). Recognition of VSV-CARMA1 by the CARMA1 antibody, but not the VSV antibody, was blocked by preincubation with the recombinant GST-CARD construct used for immunization. In addition, the CARMA1 antibody detected endogenous CARMA1 and VSV-tagged CARMA1 in retrovirally mock- or VSV-CARMA1-transduced Jurkat cells, respectively (**Fig. 1b**).

Using AL220, we analyzed whether CARMA1 physically associated with the TCR-CD3 complex upon anti-CD3 triggering in Jurkat clones that had been stably transfected with a mock or VSV-CARMA1 expression plasmid (**Fig. 1c**). The cells were left unstimulated or stimulated with anti-CD3 for various times, lysed in a 1% Brij 96 lysis buffer and the TCR-CD3 complex was recovered from cellular lysates with protein G beads (**Fig. 1c**). Analysis of the precipitated TCR-CD3 complexes with anti-phosphotyrosine revealed the rapid and transient appearance of tyrosine-phosphorylated CD3 $\epsilon$  and  $\zeta$  chains and the Syk family kinase ZAP-70, which was consistent with published data<sup>25,26</sup>. In addition, stimulation with anti-CD3 induced an association of both

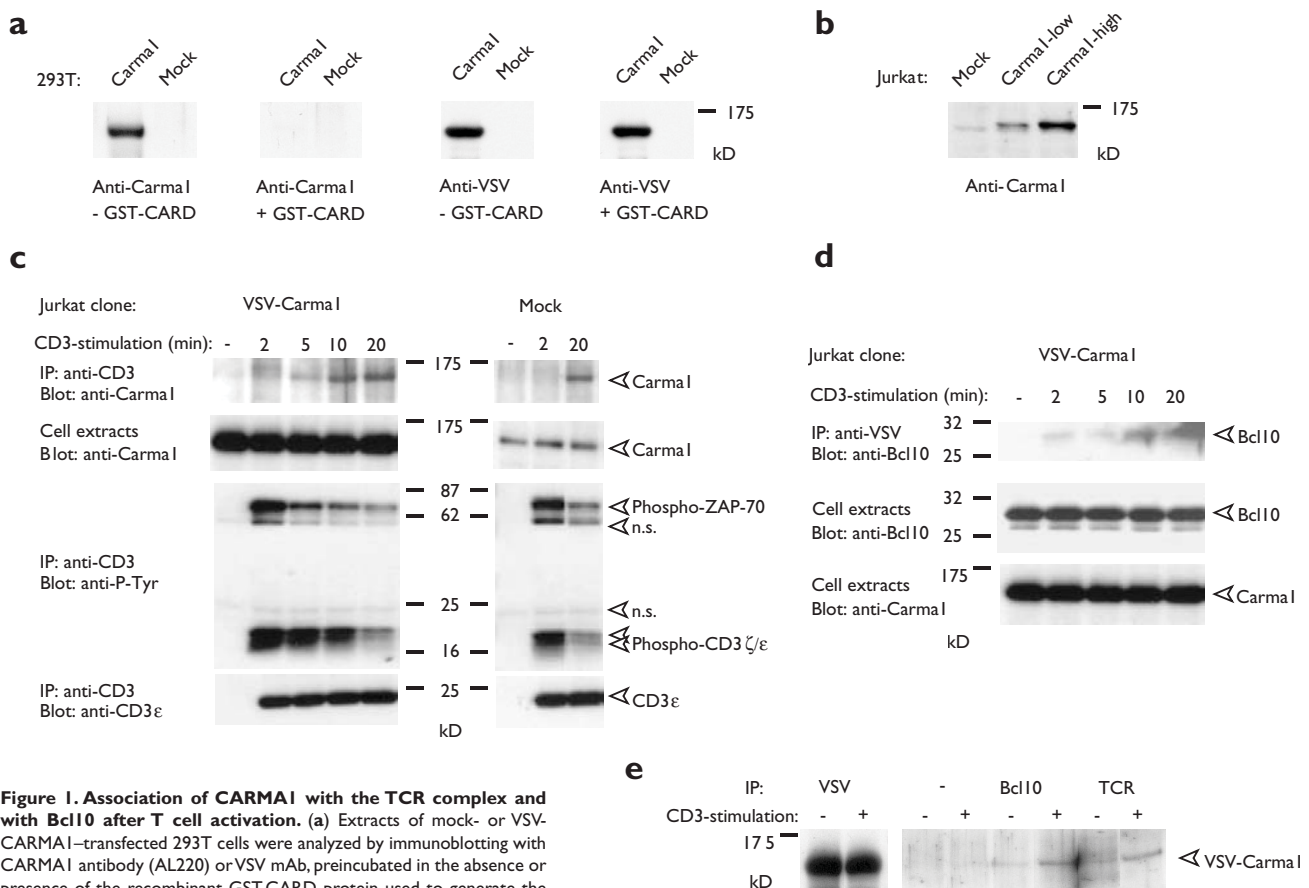
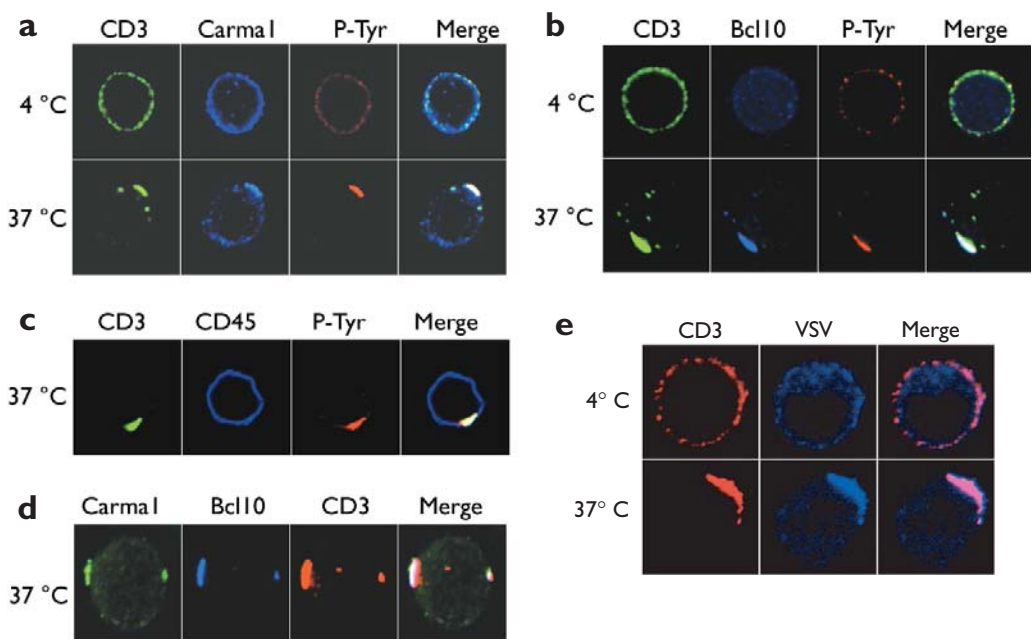


**Figure 1. Association of CARMA1 with the TCR complex and with Bcl10 after T cell activation.** (a) Extracts of mock- or VSV-CARMA1-transfected 293T cells were analyzed by immunoblotting with CARMA1 antibody (AL220) or VSV mAb, preincubated in the absence or presence of the recombinant GST-CARD protein used to generate the CARMA1 antibody. (b) Lysates of Jurkat cells, retrovirally transduced with a mock construct or with a VSV-Carma1 + GFP construct (and subsequently sorted by FACS for low and high expressors of GFP) were analyzed by immunoblotting with CARMA1 antibody (AL220). (c) Jurkat cells (VSV-CARMA1- and mock-transfected clones) were stimulated with CD3 mAb, lysed and the TCR complex was recovered by incubation with protein G sepharose. Immunoprecipitates (IP) and postnuclear lysates (cell extracts) were analyzed by immunoblotting. In the case of anti-CARMA1 immunoblots, a longer exposure was used for the mock-transfected than for the VSV-CARMA1-expressing clone. Similar results were obtained in three independent experiments. (d) Jurkat cells stably transfected with VSV-CARMA1 were stimulated and lysed as in c, and VSV-CARMA1 was recovered by incubation with anti-VSV agarose. Immunoprecipitates and postnuclear lysates were analyzed by immunoblotting. Similar results were obtained in two independent experiments. (e) Jurkat cells stably transfected with VSV-CARMA1 were stimulated with CD3 mAb for 15 min and lysed in 1% NP-40 lysis buffer. Immunoprecipitation was done with various antibodies and analyzed by anti-CARMA1 immunoblot. A shorter exposure was used for anti-VSV.

**Figure 2. Colocalization of CARMA1 and Bcl10 with the TCR after CD3-aggregation.** Human T cells (clone 6396p5.1.2) were incubated with CD3 mAb for 20 min on ice, followed by incubation with secondary goat anti-mouse for 15 min at 4 °C or 37 °C. Cells were stained for CD3 (green), phosphotyrosine (red) and CARMA1 (a), Bcl10 (b) or CD45 (c) (blue) and analyzed by confocal microscopy. (d) Aggregation was induced as in a, and cells were stained for CD3 (red), CARMA1 (green) and Bcl10 (blue). (e) Jurkat cells that were stably expressing VSV-CARMA1 were treated as in (a–d) and stained for CD3 (red) and VSV (blue). Images are representative of at least three independent experiments and colocalization was observed for most of the cells that showed a clear CD3-aggregation.



VSV-tagged CARMA1 and endogenous CARMA1 with the TCR-CD3 complex (Fig. 1c). This association appeared slow compared to the rapid association of phosphorylated ZAP-70 and reached a maximum 10–20 min after TCR-triggering (Fig. 1c and data not shown).

In cellular overexpression and two-hybrid systems, CARMA1 binds to Bcl10 *via* CARD-CARD interactions<sup>16,18</sup>. Therefore we next assessed whether TCR stimulation would induce binding of Bcl10 to CARMA1

by immunoprecipitating VSV-tagged CARMA1 from unstimulated or anti-CD3-treated Jurkat cells (Fig. 1d). In resting T cells, no association of Bcl10 with CARMA1 was detected. In contrast, anti-CD3 stimulation induced the association of a proportion of Bcl10 with CARMA1 that was slightly increased over the 20-min duration of TCR triggering. We next analyzed whether similar interactions were detectable using a 1% NP-40-containing lysis buffer, in which the TCR dissociates from the

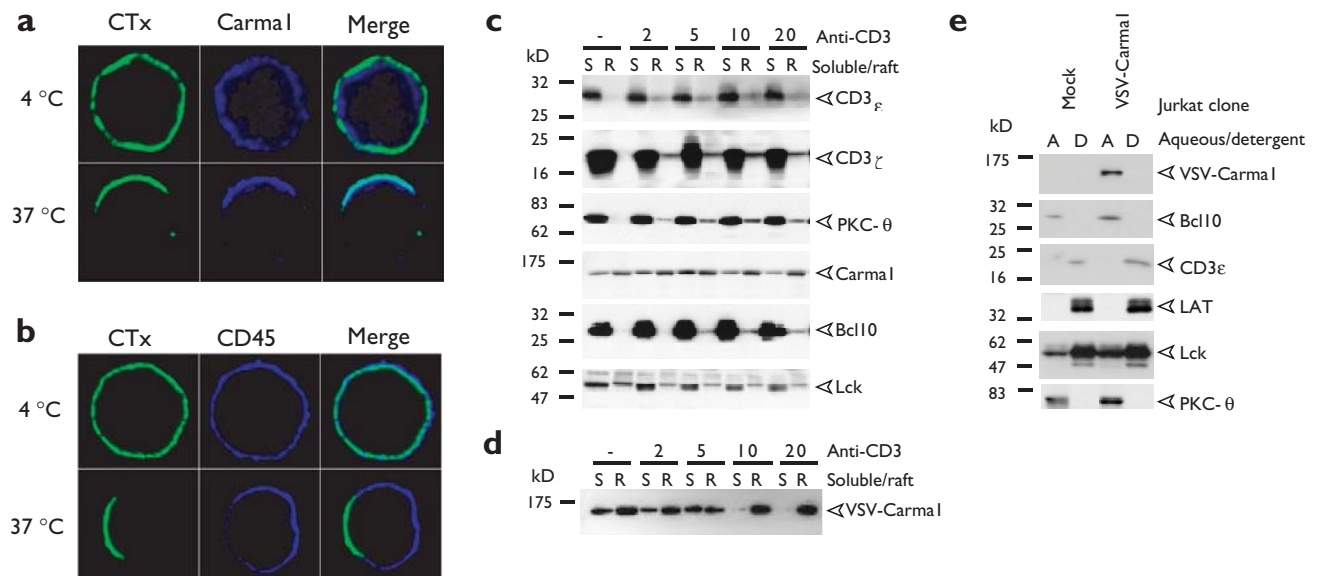


**Figure 3. Differential lipid raft localization of CARMA1 and Bcl10 in resting and CD3-triggered T cells.** (a,b) Human T cells (clone 6396p5.1.2) were incubated with FITC-CTx for 20 min on ice, followed by incubation with an anti-CTx for 15 min at 4 °C or 37 °C. Cells were analyzed for FITC-CTx-stained GM1 ganglioside (green) and CARMA1 or CD45 (blue) by confocal microscopy. Images are representative of at least three independent experiments. (c,d) Jurkat cells were activated with CD3 mAb and protein distribution of lipid raft (R) or non-raft (S) fractions was analyzed by detergent fractionation and immunoblotting in nontransfected (c) or stably VSV-CARMA1-transfected (d) Jurkat cells. (e) The subcellular distribution of CARMA1 was analyzed by Triton X-114 extraction of Jurkat cells stably transfected with VSV-CARMA1 or mock plasmid, and detergent (D) and aqueous (A) fractions were analyzed by immunoblotting. Similar results were obtained in two independent experiments.

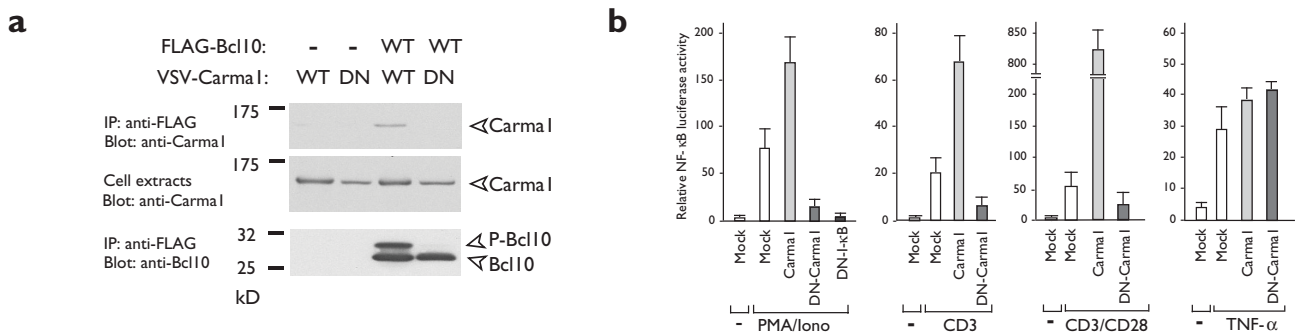


**Figure 4. Inhibitory effect of CARD-mutated CARMA1 on TCR-mediated NF-κB activation and IL-2 production.** (a) 293T cells were transfected with expression plasmids for FLAG-Bcl10 and VSV-tagged wild-type or DN CARMA1 (L39R CARD-mutated); then anti-FLAG-Bcl10 immunoprecipitates and postnuclear extracts were analyzed by immunoblotting. Coexpression of CARMA1 with Bcl10 induced the formation of a phosphorylated form of Bcl10 (P-Bcl10), as has been described<sup>16</sup>. (b) Jurkat cells, transfected with a NF-κB luciferase reporter plasmid together with mock, wild-type CARMA1, DN CARMA1 or DN (non-phosphorylatable) IκB expression constructs, as indicated, were stimulated for 3 h with PMA + ionomycin, coated CD3 mAb, CD3 and CD28 mAbs or recombinant human TNF-α; then cell lysates were analyzed for NF-κB-dependent luciferase activity. (c) Retrovirally mock- or DN CARMA1-transduced Jurkat cells were analyzed for PMA + ionomycin- or anti-CD3-induced NF-κB-dependent luciferase activity as in b. (d) Retrovirally mock- or DN CARMA1-transduced Jurkat cells were analyzed for CD3 mAb- or CD3 and CD28 mAb-induced IL-2 production. Results are representative of three independent experiments.

CD3 chains. Under these experimental conditions, CD3-stimulation induced the association of VSV-tagged CARMA1 with Bcl10 and with the TCR (Fig. 1e). Together, these results showed that TCR triggering induces a physical association of CARMA1 with Bcl10 and, directly or indirectly, with the TCR complex.

To investigate these activation-induced interactions in intact cells, we analyzed the localization of CARMA1 and Bcl10 in resting and TCR-triggered cells of a human T cell clone by confocal microscopy. In unstimulated T cells, CARMA1 showed plasma membrane and diffuse submembrane cytoplasmic staining (Fig. 2a), whereas Bcl10 showed a slightly granular staining that was detected predominantly in the cytosol (Fig. 2b). CD3 aggregation induced the colocalization of most of the cellular CARMA1 and Bcl10 with the CD3 aggregates together with an enrichment of tyrosine-phosphorylated proteins (Fig. 2a,b). Colocalization of Bcl10 and CARMA1 with CD3 was transient and reached an optimum about 15–20 min after cross-linking (data not shown). In contrast to CARMA1 and Bcl10, no colocalization was observed for CD45 (Fig. 2c), which was consistent with published reports<sup>27,28</sup>. Simultaneous staining for endogenous Bcl10 and CARMA1 confirmed colocalization of both proteins with the TCR aggregates (Fig. 2d). Colocalization of CARMA1 with CD3 was also seen with a second antiserum that recognized the COOH terminus of CARMA1 and, when VSV-CARMA1-transfected Jurkat cells were used instead of T cell clones, with a VSV monoclonal antibody (mAb) (Fig. 2e and data not shown). Together with the coimmunoprecipitation experiments, these findings indicated that CARMA1 and Bcl10 translocate to the TCR complex after anti-CD3 activation.

#### Lipid raft partitioning of CARMA1 and Bcl10

TCR engagement induces the translocation of the TCR complex and multiple other signaling molecules into lipid rafts<sup>4,5,7,8,29</sup>. Lipid rafts are enriched in the glycosphingolipid GM1, which can be specifically

detected by confocal microscopy with fluorescently labeled cholera toxin B (CTx)<sup>4,27,29,30</sup>. Cross-linking of GM1-bound CTx with a secondary antibody induces the formation of lipid raft patches that initiate signaling events similar to TCR stimulation<sup>27,30</sup>.

To analyze whether CARMA1 localizes to such lipid raft patches, cells from a human T cell clone were incubated with fluorescein isothiocyanate (FITC)-labeled CTx. At 4 °C, staining of GM1 was mainly detected at the plasma membrane (Fig. 3a,b), whereas CARMA1 was expressed, in a diffuse manner, at the plasma membrane and in a submembrane cytoplasmic compartment (Fig. 3a). Within 15 min of cross-linking, a large fraction of CARMA1 and most GM1 had translocated to lipid raft patches (Fig. 3a,b, compare 4 °C and 37 °C). In contrast, CD45 was excluded from CTx patches, in agreement with published data<sup>27</sup>. Similar data were obtained with Jurkat cells (data not shown).

To further investigate whether CARMA1 partitions into lipid rafts, Jurkat cells were either left unstimulated or stimulated for various times with CD3 mAb; proteins were separated into a Triton X-100-soluble and a Triton X-100-insoluble β-octylglucoside-soluble lipid raft fraction<sup>29,31</sup>. In unstimulated cells, CARMA1 was constitutively present in lipid rafts for both endogenous (Fig. 3c) and exogenous VSV-tagged CARMA1 (Fig. 3d). In contrast, Bcl10 was excluded from lipid rafts in resting cells. Consistent with published data<sup>5,7,10,29</sup>, PKC-θ and CD3 were also absent from lipid rafts, whereas Lck partially distributed to lipid rafts in unstimulated cells. TCR stimulation induced an enrichment of CARMA1 in lipid rafts, which was even more pronounced in Jurkat cells overexpressing VSV-tagged CARMA1 (Fig. 3a–d). This was paralleled by the translocation of a small fraction of Bcl10 into the lipid raft fraction after anti-CD3 stimulation. Similarly, CD3e, CD3ζ and PKC-θ translocated to the lipid raft fraction in a TCR stimulation-dependent manner. Thus, CARMA1 was constitutively associated with lipid rafts in T cells, and its further



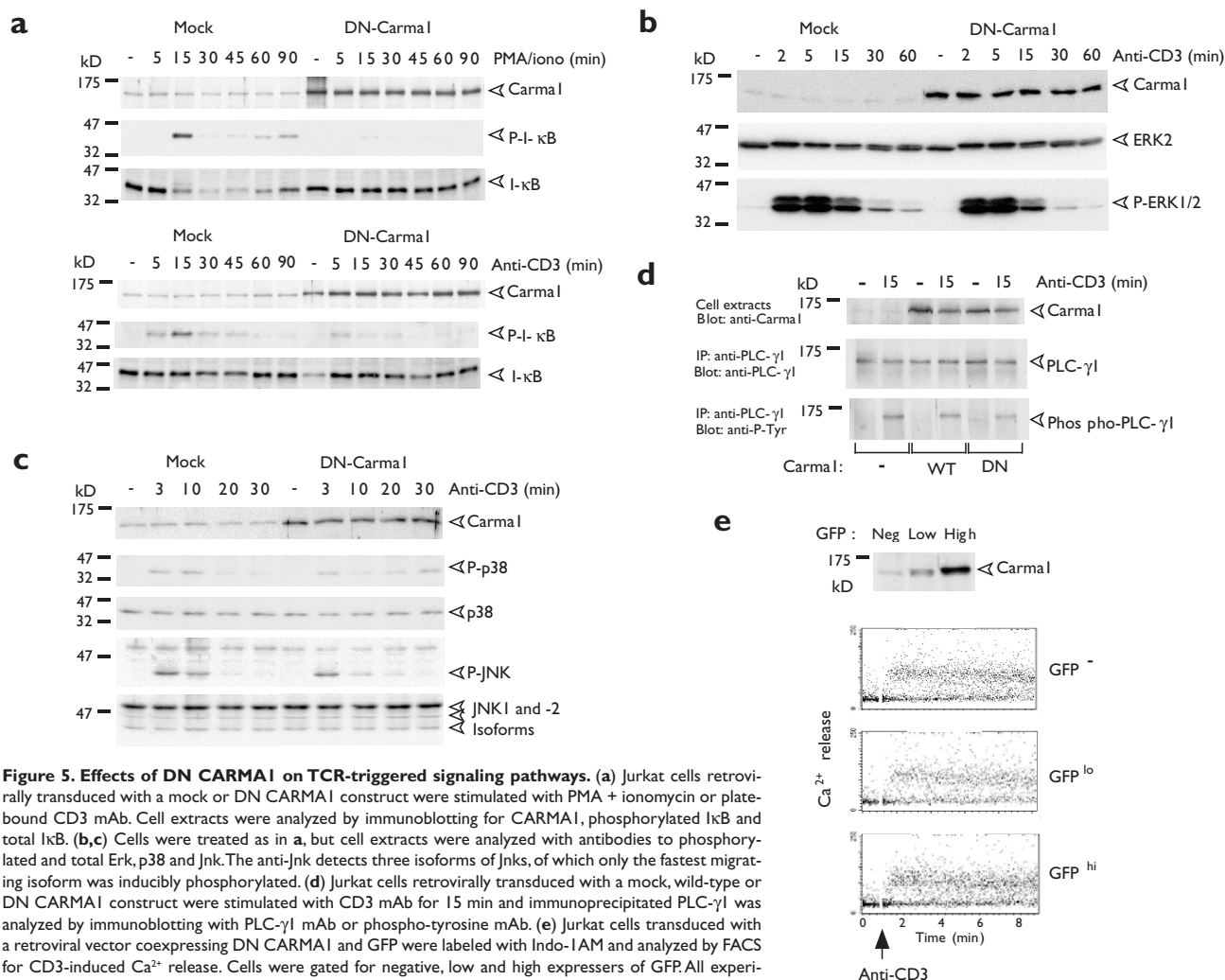


**Figure 5. Effects of DN CARMA1 on TCR-triggered signaling pathways.** (a) Jurkat cells retrovirally transduced with a mock or DN CARMA1 construct were stimulated with PMA + ionomycin or plate-bound CD3 mAb. Cell extracts were analyzed by immunoblotting for CARMA1, phosphorylated IκB and total IκB. (b,c) Cells were treated as in a, but cell extracts were analyzed with antibodies to phosphorylated and total Erk, p38 and Jnk. The anti-Jnk detects three isoforms of Jnks, of which only the fastest migrating isoform was inducibly phosphorylated. (d) Jurkat cells retrovirally transduced with a mock, wild-type or DN CARMA1 construct were stimulated with CD3 mAb for 15 min and immunoprecipitated PLC-γ1 was analyzed by immunoblotting with PLC-γ1 mAb or phospho-tyrosine mAb. (e) Jurkat cells transduced with a retroviral vector coexpressing DN CARMA1 and GFP were labeled with Indo-1AM and analyzed by FACS for CD3-induced Ca<sup>2+</sup> release. Cells were gated for negative, low and high expressors of GFP. All experiments are representative of at least two independent experiments.

enrichment in lipid rafts during T cell activation was paralleled by a partial lipid raft translocation of its binding partner Bcl10.

Constitutive lipid raft association in lymphocytes has been described for proteins with a glycosyl-phosphatidyl inositol (GPI) anchor and for myristoylated and/or palmitoylated proteins<sup>4,6,32</sup>. CARMA1 lacks an apparent consensus sequence for a GPI anchor or a covalent NH<sub>2</sub>-terminal or COOH-terminal acylation. We therefore reasoned that lipid raft targeting of CARMA1 may be due to intramolecular acylation or mediated indirectly through interaction with a constitutive lipid raft component. To differentiate between these possibilities, we analyzed the repartition of CARMA1 into the aqueous and detergent phase with Triton X-114, a detergent that solubilizes transmembrane, GPI-anchored and lipid-modified proteins<sup>24,33,34</sup> (Fig. 3e). As expected, CD3ε and LAT were recovered from the detergent phase, as well as a fraction of Lck, which is partially targeted to the plasma membrane by NH<sub>2</sub>-terminal myristoylation and palmitoylation<sup>35</sup>. In contrast, both CARMA1 and Bcl10 partitioned exclusively into the aqueous phase (Fig. 3e). These results argued against a lipid modification of CARMA1 and suggested that CARMA1 is targeted to membrane lipid rafts by binding to an integral lipid raft component.

### TCR-induced NF-κB activation and IL-2 production

We generated a CARD point mutant (L39R) of CARMA1 that, in contrast to wild-type CARMA1, did not bind to Bcl10 and was therefore predicted to act as a dominant negative (DN) inhibitor of CARMA1 function (Fig. 4a). We then investigated the impact of transiently expressed wild-type and DN CARMA1 on NF-κB activation by phorbol 12-myristate 13-acetate (PMA) + ionomycin or anti-CD3 treatment of Jurkat cells. Cells were transfected with CARMA1 or mock constructs together with a NF-κB-dependent luciferase reporter plasmid. Stimulation of the mock-transfected cells with PMA + ionomycin caused a ~80-fold induction of NF-κB activity that was inhibited by expression of a DN IκB construct (Fig. 4b). NF-κB induction by PMA + ionomycin was increased by cotransfection of wild-type CARMA1, whereas the DN CARMA1 mutant had an inhibitory effect. Similar results were obtained for anti-CD3- or anti-CD3 and anti-CD28-induced NF-κB activation, which was increased in the presence of wild-type CARMA1, but considerably reduced by DN CARMA1. Thus, the Bcl10 binding-defective form of CARMA1 acts as a DN inhibitor of TCR-induced NF-κB activation. In contrast, wild-type and mutant CARMA1 did not affect TNF-α-induced NF-κB activation.

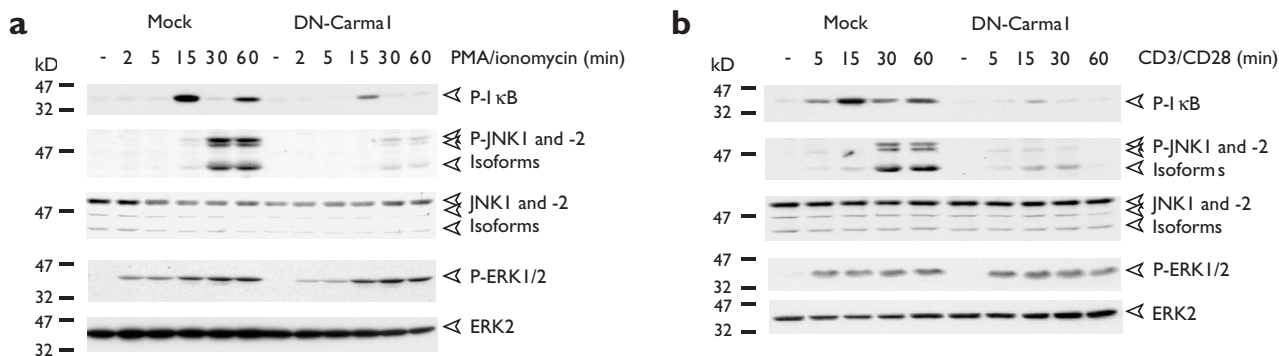


**Figure 6. Effects of DN CARMA1 on PMA + ionomycin and CD28 costimulation–induced signaling pathways.** Jurkat cells retrovirally transduced with a mock- or DN CARMA1 construct were stimulated with PMA + ionomycin (a) or plate-bound CD3 and CD28 mAbs (b) and cell extracts were analyzed by immunoblotting for phosphorylated IκB and phosphorylated and total Erk and Jnk. Results are representative of two independent experiments.

To biochemically analyze the effect of DN CARMA1 on TCR signaling pathways, we generated Jurkat cell populations that were stably transduced with wild-type or DN CARMA1 using a retroviral approach. CD3- or PMA + ionomycin–induced NF-κB activation was inhibited in the Jurkat cell population expressing the DN CARMA1 construct (Fig. 4c). NF-κB is one of the critical transcription factors regulating IL-2 induction in activated T cells<sup>36</sup>. We therefore next tested whether DN CARMA1 affected the production of this cytokine in response to T cell activation. DN CARMA1 completely inhibited IL-2 secretion induced by anti-CD3 treatment, whereas it moderately reduced anti-CD3 and anti-CD28–induced IL-2 secretion (Fig. 4d).

To further investigate how DN CARMA1 inhibited NF-κB activation molecularly, we next tested the effect of DN CARMA1 on PMA + ionomycin– or anti-CD3–induced phosphorylation of IκB and found it inhibited both (Fig. 5a). For the strong signal provided by PMA + ionomycin treatment, IκB phosphorylation correlated with subsequent IκB degradation, which was inhibited by DN CARMA1 (Fig. 5a). In contrast, expression of wild-type or DN CARMA1 did not appear to affect other TCR signaling pathways, such as anti-CD3–induced activation of the Erk (extracellular signal–regulated kinase), p38 and Jnk pathways, the tyrosine phosphorylation of PLC-γ1 or Ca<sup>2+</sup> mobilization (Fig. 5b–e and data not shown).

Optimal Jnk activation by the TCR requires costimulation of CD28 and can be mimicked by PMA + ionomycin<sup>37</sup>. Both IκB phosphorylation and Jnk activation by PMA + ionomycin or by anti-CD3 + anti-CD28 was inhibited by DN CARMA1, whereas Erk activation by these stimuli was unaffected (Fig. 6a,b). Thus, CARMA1 plays a critical role in TCR-induced NF-κB activation and CD28 costimulation–dependent Jnk activation.

## Discussion

Here, we provide evidence for the importance of CARMA1 in TCR-mediated NF-κB activation. We show that CARMA1 is a lipid raft–associated molecule that interacts with Bcl10 and the TCR complex upon TCR triggering. The Src family tyrosine kinase Lck is essential for lipid raft translocation of the TCR<sup>31</sup>. Thus, initial Lck activation may be required for the observed interaction of the TCR with lipid raft–associated CARMA1. It is unlikely, however, that the association of CARMA1 with the TCR complex merely relies on lipid raft colocalization, as translocation of the activated TCR complexes into lipid rafts was detectable as early as 2 min after anti-CD3 triggering. In contrast the TCR–CARMA1 association was optimal about 15–20 min after TCR

engagement. The association of CARMA1 with the TCR complex may be indirect and mediated by one or more constitutively lipid raft–associated factor(s). This hypothesis is supported by the absence of CARMA1 from the Triton X-114 detergent fraction of liposoluble proteins, which argues against a lipid modification of CARMA1 and instead suggests that it partitions into lipid rafts *via* a protein–protein interaction that does not resist the Triton X-114 extraction.

Association with membrane proteins is a general feature of MAGUKs and is thought to be conferred by the conserved COOH-terminal array comprising the PDZ, SH3, linker and GUK motifs. The PDZ motif of CARMA1 represents an attractive candidate for membrane and, potentially, lipid raft targeting of CARMA1, as PDZ domains of other MAGUKs bind primarily to the cytoplasmic tails of transmembrane proteins and membrane channels<sup>20,21</sup>.

The CARD motif–containing ortholog of Bcl10 and CARMA1, vE10, is a lipid-modified protein that associates with the plasma membrane, thereby inducing membrane recruitment of Bcl10. vE10 potentially activates NF-κB through a mechanism that is dependent on its capacity to bind Bcl10 and to incorporate into the plasma membrane<sup>24</sup>. Thus, vE10 may represent a functional ortholog of CARMA1, by anchoring Bcl10 to the plasma membrane.

The recruitment of Bcl10 to the TCR complex by CARMA1 is supported by several lines of evidence. First, TCR triggering induced the coimmunoprecipitation of Bcl10 with a VSV-tagged form of CARMA1 and recruitment of Bcl10 to the lipid raft fraction with similar kinetics. In addition, Bcl10 and CARMA1 colocalized with aggregated CD3 in confocal experiments. Finally, a CARD point mutant of CARMA1, that was unable to bind Bcl10, acted as a DN inhibitor of TCR-induced NF-κB activation. Together, our data are consistent with the idea that Bcl10 acts downstream of CARMA1 in the TCR-triggered pathway that leads to NF-κB activation. However, these findings do not exclude the involvement of other CARD-binding partner(s) of CARMA1 in TCR-induced NF-κB activation. It is likely that the CARMA1–Bcl10 interaction we report here is regulated by TCR-dependent modifications and/or conformational changes in the binding partner(s) that renders the CARD motif(s) accessible for binding.

Bcl10 binds the CARD motifs of CARMA1, CARMA2 and CARMA3<sup>16–19</sup> and may act as a general adaptor molecule downstream of all three CARMA paralogs for several reasons. First, NF-κB activation by PMA + ionomycin or by CARMA2 or CARMA3 overexpression is inhibited in embryonic fibroblasts of Bcl10-deficient mice<sup>17</sup>. Second, non-Bcl10–binding CARD-deletion mutants of all three

CARMA paralogs fail to induce NF- $\kappa$ B in overexpression systems<sup>17,18</sup>. Third, wild-type Bcl10, but not CARD-mutated Bcl10 synergizes with CARMA3 in NF- $\kappa$ B activation<sup>17</sup>. Finally, a CARD-deletion mutant of CARMA3 inhibits PKC- $\alpha$ - and PKC- $\epsilon$ -induced NF- $\kappa$ B activation in a 293T cell transfection system<sup>17</sup>. These findings are consistent with the results we report here and suggest that the CARMA paralogs act upstream of Bcl10 in various signaling pathways that activate the NF- $\kappa$ B pathway *via* diacylglycerol (DAG)-inducible PKCs.

The exact molecular link between CARMA1, Bcl10 and the downstream IKK components controlling NF- $\kappa$ B activation in T cells is unclear. IKK activation can be mediated by tumor necrosis factor receptor (TNFR)-associated factor (TRAF) proteins, which are key components in various NF- $\kappa$ B activating pathways<sup>38</sup>. For example, TRAF2 recruits IKK $\alpha$  and IKK $\beta$  to the TNFR1<sup>39</sup>, whereas TRAF6 mediates interleukin 1 (IL-1) and lipopolysaccharide-induced NF- $\kappa$ B activation by recruitment and ubiquitin-dependent activation of the IKK-activating kinase transforming growth factor- $\beta$ -activated kinase (TAK1)<sup>40</sup>. Bcl10 interacts with TRAF1, TRAF2 and TRAF5<sup>41,42</sup> and it is therefore possible that the IKK complex is recruited to Bcl10 *via* one of the TRAFs.

The paracaspase MLT (also known as MALT1) is likely to be another key signal transducer linking Bcl10 to activation of the IKK complex<sup>17,43</sup>. Two distinct chromosomal translocations involving the genes encoding Bcl10 and MLT are implicated in the pathogenesis of MALT B cell lymphoma<sup>14,15,44-46</sup>; this suggests that Bcl10 and MLT are part of the same signaling pathway that leads to constitutive NF- $\kappa$ B activation and lymphoma formation. Indeed, Bcl10 binds to MLT<sup>43,47</sup> and this association, as well as the presence of the caspase-like domain of MLT, are required for the synergistic activation of NF- $\kappa$ B by Bcl10 and MLT<sup>47</sup>. Together with the findings described here, these data suggest that the B cell and T cell antigen receptor signals are relayed to the NF- $\kappa$ B-activating IKK complex *via* a pathway that depends on CARMA1, Bcl10, MLT and/or TRAF family members.

Exogenous expression of a DN version of CARMA1 blocked NF- $\kappa$ B activation after TCR triggering or PMA-dependent PKC activation in T cells. Similar findings have been reported for CARMA3<sup>17</sup>. However, CARMA1 is predominantly expressed in lymphocytes, whereas CARMA2 shows predominant expression in placenta and CARMA3 has a relatively wide tissue distribution with little or no expression of mRNA in lymphoid tissues and PBLs<sup>17-19</sup>. These findings suggest that CARMA1 plays a critical and nonredundant role for the transmission of the NF- $\kappa$ B signal downstream of the TCR and of PKC- $\theta$ .

We found that DN CARMA1 did not affect Jnk activation by the TCR alone, but it inhibited this pathway under conditions of CD3 and CD28 costimulation or when the TCR was bypassed by PMA + ionomycin, conditions that optimally activate the Jnk pathway<sup>37</sup>. PKC- $\theta$  has been suggested to integrate TCR-CD28 costimulatory signals, as a DN form of PKC- $\theta$  inhibits Jnk activation in Jurkat T cells<sup>48</sup>. Our observations are consistent with these findings and suggest a role for CARMA1 in Jnk activation downstream of CD28 and PKC- $\theta$ . However, it remains to be seen whether this observation is specific to the use of Jurkat T cells, as Jnk activation by CD3 and CD28 coengagement is unaffected in primary T cells of PKC- $\theta$ -deficient mice<sup>12</sup>.

DN CARMA1 completely inhibited CD3-induced IL-2 production, but only moderately inhibited IL-2 production in anti-CD3 and anti-CD28-stimulated T cells. This observation is compatible with the idea that coengagement of CD28 synergizes with TCR signal transduction at various points in the signaling cascade<sup>49</sup>. The inhibitory role played by DN CARMA1 in TCR-induced IL-2 production may be either decreased or by-passed by the engagement of CD28-specific pathways.

The generation of CARMA1-deficient mice and the investigation of

CARMA1-interacting proteins will help to further elucidate the precise molecular function of CARMA1 in antigen receptor-induced signaling pathways and lymphocyte proliferation.

## Methods

**Cell culture and transfection.** Jurkat cells (J77 clone 20, a gift of O. Acuto, Paris) were grown in RPMI 1640 medium supplemented with 10% heat-inactivated fetal calf serum (FCS) and penicillin and streptomycin (100  $\mu$ g/ml of each). For the generation of VSV-CARMA1-expressing stable Jurkat clones,  $8 \times 10^6$  Jurkat cells were transfected with mock plasmid (SR $\alpha$ puro, 20  $\mu$ g) or a VSV-CARMA1 expression construct in SR $\alpha$ puro (a gift of R.-P. Sékaly, Montreal) by electroporation at 250 kV and 960  $\mu$ F. Puromycin-resistant stable clones were selected with puromycin (3  $\mu$ g/ml, Sigma, Buchs, Switzerland). Jurkat populations expressing VSV-tagged wild-type or CARD mutant (L39R) CARMA1 together with GFP were obtained by retroviral infection of the cells with the respective constructs in MSCV-IRES-GFP vector (a gift of J. Schwaller, Geneva) and subsequent FACS sorting for GFP-expressing cells.

**Reporter assays.** Jurkat cells ( $8 \times 10^6$ ) were transiently transfected by electroporation at 250 kV and 960  $\mu$ F with CARMA1, IkB or mock constructs (20  $\mu$ g), SV40 large T expression vector (5  $\mu$ g), an NF- $\kappa$ B *firefly* luciferase (5  $\mu$ g) and a *renilla* luciferase reporter plasmid (1  $\mu$ g, Promega, Wallisellen, Switzerland). Cells ( $4 \times 10^6$ ) were treated for 4 h with plate-bound CD3 mAb (TR66 or OKT3, 10  $\mu$ g/ml), CD3 mAb (1  $\mu$ g/ml) and CD28 mAbs (10  $\mu$ g/ml, CD28.2, Coulter-Immunotech, Marseille, France), PMA (20 ng/ml) + ionomycin (1  $\mu$ M) or recombinant human TNF- $\alpha$  (10  $\mu$ g/ml, Apotech Biochemicals, Switzerland) 24–32 h after transfection. Cells were washed twice with PBS and lysed in 50  $\mu$ l of Triton X-100, glycylglycine lysis buffer (1% Triton X-100, 25 mM glycylglycine at pH 7.8, 14 mM MgSO<sub>4</sub>, 4 mM EGTA and 1 mM DTT). Aliquots of cell lysates (10  $\mu$ l) were analyzed for luciferase activities with the Dual Luciferase Reporter Assay (E1910, Promega) on a Turner Design TD-20/20 Laboratory Fluorometer (Sunnyvale, CA), according to the manufacturer's protocol.

**IL-2 assay.** Jurkat T cells ( $10^6$  cells/0.5 ml) were stimulated with or without immobilized CD3 mAb (OKT3, 10  $\mu$ g/ml) or with OKT3 and CD28.2 mAbs (1 and 10  $\mu$ g/ml, respectively) in 24-well microtiter plates for 24 h at 37 °C. IL-2 concentration in the supernatants was determined by ELISA (R&D systems, Oxford, UK), according to the manufacturer's instructions.

**T cell activation, immunoprecipitation and immunoblotting.** For immunoprecipitations, Jurkat cells (wild-type, mock-transfected or a stable clone expressing VSV-tagged CARMA1) were incubated at  $7 \times 10^7$  cells/ml in the absence or presence of CD3 mAb (TR66, 10  $\mu$ g/ml). Cells were washed quickly in cold Tris-NaCl (20 mM Tris-HCl at pH 7.4 and 150 mM NaCl) and lysed in 1% Brij 96 or 1% NP-40 lysis buffer containing Tris-HCl at pH 7.4 (20 mM), NaCl (150 mM), protease inhibitors (Complete, Roche, Rotkreuz, Switzerland) and phosphatase inhibitors (cocktails I and II, Sigma). Postnuclear lysates of equivalent protein content were precleared on sepharose 6B for 1 h at 4 °C. VSV-tagged CARMA1, Bcl10 and the TCR were immunoprecipitated with VSV-agarose (Sigma), anti-Bcl10 (mAb 333.1, Santa Cruz, LabForce AG, Nunningen, Switzerland) and TCR V $\beta$ 8 mAb (5 Rex-5H9, a gift of O. Acuto, Paris), respectively. Immunoprecipitates were washed twice with the corresponding 1% detergent lysis buffer and twice with 0.05% detergent lysis buffer without inhibitors. For analysis of IkB or MAPK phosphorylation, cells were stimulated with or without immobilized CD3 mAb (TR66, 10  $\mu$ g/ml), with TR66 and CD28.2 mAbs (1 and 10  $\mu$ g/ml, respectively) or with PMA (20 ng/ml) + ionomycin (1  $\mu$ M); then cell lysates prepared as described above. Immunoprecipitates and aliquots of lysates of equivalent protein content were analyzed by SDS-PAGE and immunoblotting on nitrocellulose membrane (Hybond ECL, Amersham Pharmacia Biotech, Dubendorf, Switzerland). Blocking and antibody incubations were done for 1 h at room temperature in 5% skim milk in PBS and 0.5% Tween, followed by four washes of 15 min with PBS and 0.5% Tween. Primary antibodies used for immunoblotting included CARMA1 polyclonal antiserum (AL220, generated against a GST fusion protein containing the NH<sub>2</sub>-terminal CARD motif of CARMA1) and an affinity-purified polyclonal rabbit antibody (AL114), which recognizes the NH<sub>2</sub> terminus of murine and human Bcl10<sup>24</sup>. Antibodies directed against CD3 $\epsilon$ , PKC- $\theta$ , Lck, LAT, PLC- $\gamma$ 1, Erk2 and phospho-Erk1 and Erk2 were from Santa Cruz; antibodies against total or phosphorylated IkB $\alpha$ , Jnk1 and Jnk2 and p38 were from Cell Signaling Technology (Bioconcept, Allschwil, Switzerland). Tyrosine-phosphorylated ZAP-70 and CD3 $\zeta$  chains were detected with mAb to phosphotyrosine (4G10, Upstate Biotechnology, Lake Placid, NY), in this case blocking and incubation steps were done with 1% teleostean gelatin (Sigma). Secondary goat anti-mouse, goat anti-rabbit and mouse anti-goat were from Jackson ImmunoResearch Laboratories (Milian Analytic, Geneva, Switzerland). Blots were revealed with the enhanced chemiluminescence kit (Amersham Pharmacia Biotech).

**Triton X-114 extraction.** Cells ( $\sim 5 \times 10^6$ ) were collected and extracted twice with Triton X-114<sup>33</sup>. Proteins of the aqueous and diluted detergent phases were precipitated by the addition of MeOH/CHCl<sub>3</sub> (4:1, v/v), and the resulting protein pellet was dried, resuspended in reduced SDS-PAGE sample buffer (Tris-HCl at pH 6.8 (125 mM), SDS (4% w/v), glycerol (20%)), sonicated and boiled before loading for SDS-PAGE and immunoblotting.

**Confocal microscopy.** Human T cell clone 6396p5.1.2<sup>50</sup> ( $3 \times 10^5$  cells) were washed in PBS-F (PBS with 1% FCS) and incubated on ice for 20 min with CD3 mAb (OKT3, 10  $\mu$ g/ml).



Cells were washed three times with PBS-F and incubated either at 37 °C or at 4 °C with a secondary goat anti-mouse (Jackson ImmunoResearch) in PBS-F for 15 min. The cells were laid on poly(L)lysine-coated slides for 5 min at 37 °C, fixed for 10 min with 3% paraformaldehyde, permeabilized for 5 min with 0.1% Triton-X100 and stained with the following antibodies: Bcl10 mAb (331.3, Santa Cruz), anti-phosphotyrosine (PY99, Santa Cruz), rabbit antiserum to CARMA (AL220 and AL222, generated against GST fusion proteins containing the NH<sub>2</sub>-terminal CARD and the COOH-terminal GUK domain of CARMA1, respectively), CD45 mAb (10G10, a gift of F. Spertini, Lausanne, Switzerland) and VSV mAb (P5D4, Roche). Primary antibodies were revealed with secondary goat antibodies conjugated to FITC, Cy5 or Cy3.

For raft-aggregation experiments, T cells (clone 6396p5.1.2) were incubated with FITC-CTx (5 µg/ml, Sigma) for 20 min on ice, followed by incubation with goat anti-CTx (Calbiochem, Juro, Luzern, Switzerland) for 15 min either at 4 °C or at 37 °C. Cells were fixed, permeabilized and stained with either CARMA antibody or with CD45 mAb followed by secondary goat antibodies conjugated to Cy5. The samples were mounted in 80% glycerol-PBS containing 2.5% 1,4-diazabicyclo (2.2.2) octane (DABCO, Fluka, Buchs, Switzerland) and were examined with a Carl Zeiss LSM 510 confocal microscope (Carl Zeiss, Oberkochen, Germany).

**Lipid raft isolation.** Lipid rafts were prepared as described<sup>29</sup>. Briefly, Jurkat T cells (8 × 10<sup>6</sup>) were lysed on ice for 20 min in 200 µl of 1% Triton X-100 in MN buffer (25 mM MES and 150 mM NaCl at pH 6.5) supplemented with benzamide (10 µg/ml), antipain (2 µg/ml) and leupeptin (1 µg/ml). The cell lysate was homogenized with a loose-fitting Dounce homogenizer (10 strokes) and spun at 500g for 7 min at 4 °C. The post-nuclear supernatant was centrifuged at 100,000g for 50 min at 4 °C. The 100,000g supernatant is referred to as the detergent soluble phospholipid membrane and cytosolic fraction. The 100,000g pellet was solubilized in 200 µl of β-octyl-gluco-pyranoside buffer (β-octyl-gluco-pyranoside (50 mM, Sigma) in Tris (20 mM) and NaCl (500 mM at pH 8.0) containing protease inhibitors, and insoluble material was removed by centrifugation for 12 min at 10,000g. This β-octyl-gluco-pyranoside-soluble fraction is referred to as lipid raft fraction.

**Calcium mobilization assays.** Jurkat cells were washed once with RPMI medium containing 1% FCS (RPMI 1%) and incubated at 5 × 10<sup>6</sup> cells/ml for 40 min at 37 °C in RPMI 1% with Indo-1AM (1 µM, Sigma) in the dark. Cells were washed once with RPMI 1%, adjusted to a final concentration of 2 × 10<sup>6</sup>–3 × 10<sup>6</sup> cells/ml in RPMI with 5% FCS, and cell suspensions were maintained on ice in the dark. Before induction of calcium mobilization, cell suspensions were placed in a prewarmed FACS sample chamber at 37 °C for 2 min, and Ca<sup>2+</sup> release was induced by simultaneous addition of CD3 mAb (TR66, 10 µg/ml) and goat anti-mouse (Sigma) at 5 µg/ml after 1 min of recording. Fluorescence was excited at 350 nm and emission of fluorescence at wavelengths of 405 and 525 nm was recorded for 512 s.

#### Acknowledgments

Supported by grants from the Swiss Cancer League (to M.T. and J.T.) and by the Swiss Academy of Medical Sciences (to O.G., C.B. and D.L.) were supported by grants from the Swiss National Science Foundation and the Giorgi Cavaglieri Foundation; S.V. was supported by grants from La Ligue contre le Cancer, La Fondation pour la Recherche Médicale and the Giorgi Cavaglieri Foundation. We thank S. Levrant for technical assistance, 842P. Zaech for help with FACS analysis and K. Burns, F. Martinon and M. Thuru for critical review of the manuscript.

#### Competing interests statement

The authors declare that they have no competing financial interests.

1. Kane, L. P., Lin, J. & Weiss, A. Signal transduction by the TCR for antigen. *Curr. Opin. Immunol.* **12**, 242–249 (2000).
2. Gerondakis, S., Grumont, R., Rourke, I. & Grossmann, M. The regulation and roles of Rel/NF-κB transcription factors during lymphocyte activation. *Curr. Opin. Immunol.* **10**, 353–359 (1998).
3. Cantrell, D. T. Cell antigen receptor signal transduction pathways. *Annu. Rev. Immunol.* **14**, 259–274 (1996).
4. Janes, P.W., Ley, S. C., Magee, A. I. & Kabouridis, P.S. The role of lipid rafts in T cell antigen receptor (TCR) signalling. *Semin. Immunol.* **12**, 23–34 (2000).
5. Zhang, W., Tribble, R. P. & Samelson, L. E. LAT palmitoylation: its essential role in membrane microdomain targeting and tyrosine phosphorylation during T cell activation. *Immunity* **9**, 239–246 (1998).
6. Resh, M. D. Fatty acylation of proteins: new insights into membrane targeting of myristoylated and palmitoylated proteins. *Biochim. Biophys. Acta* **1451**, 1–16 (1999).
7. Montixi, C. et al. Engagement of T cell receptor triggers its recruitment to low-density detergent-insoluble membrane domains. *EMBO J.* **17**, 5334–5348 (1998).
8. Xavier, R., Brennan, T., Li, Q., McCormack, C. & Seed, B. Membrane compartmentation is required for efficient T cell activation. *Immunity* **8**, 723–732 (1998).
9. Khoshnan, A., Bae, D., Tindell, C. A. & Nel, A. E. The physical association of protein kinase Cθ with a lipid raft-associated inhibitor of κB factor kinase (IKK) complex plays a role in the activation of the NF-κB cascade by TCR and CD28. *J. Immunol.* **165**, 6933–6940 (2000).
10. Bi, K. et al. Antigen-induced translocation of PKCθ to membrane rafts is required for T cell activa-

- tion. *Nature Immunol.* **2**, 556–563 (2001).
11. Bi, K. & Altman, A. Membrane lipid microdomains and the role of PKCθ in T cell activation. *Semin. Immunol.* **13**, 139–146 (2001).
12. Sun, Z. et al. PKCθ is required for TCR-induced NF-κB activation in mature but not immature T lymphocytes. *Nature* **404**, 402–407 (2000).
13. Ruland, J. et al. Bcl10 is a positive regulator of antigen receptor-induced activation of NF-κB and neural tube closure. *Cell* **104**, 33–42 (2001).
14. Willis, T. G. et al. Bcl10 is involved in t(1;14)(p22;q32) of MALT B cell lymphoma and mutated in multiple tumor types. *Cell* **96**, 35–45 (1999).
15. Zhang, Q. et al. Inactivating mutations and overexpression of BCL10, a caspase recruitment domain-containing gene, in MALT lymphoma with t(1;14)(p22;q32). *Nature Genet.* **22**, 63–68 (1999).
16. Gaide, O. et al. CARMA1, a CARD-containing binding partner of Bcl10, induces Bcl10 phosphorylation and NF-κB activation. *FEBS Lett.* **496**, 121–127 (2001).
17. McAllister-Lucas, L. M. et al. Bim1, a MAGUK family member linking protein kinase C activation to Bcl10-mediated NF-κB induction. *J. Biol. Chem.* **276**, 30589–30597 (2001).
18. Bertin, J. et al. CARD11 and CARD14 are novel caspase recruitment domain (CARD)/membrane-associated guanylate kinase (MAGUK) family members that interact with BCL10 and activate NF-κB. *J. Biol. Chem.* **276**, 11877–11882 (2001).
19. Wang, L. et al. Card10 is a novel caspase recruitment domain/membrane-associated guanylate kinase family member that interacts with BCL10 and activates NF-κB. *J. Biol. Chem.* **276**, 21405–21409 (2001).
20. Fanning, A. S. & Anderson, J. M. Protein modules as organizers of membrane structure. *Curr. Opin. Cell Biol.* **11**, 432–439 (1999).
21. Dimitratos, S. D., Woods, D. F., Stathakis, D. G. & Bryant, P. J. Signaling pathways are focused at specialized regions of the plasma membrane by scaffolding proteins of the MAGUK family. *Bioessays* **21**, 912–921 (1999).
22. Ponting, C. P., Phillips, C., Davies, K. E. & Blake, D. J. PDZ domains: targeting signalling molecules to sub-membranous sites. *Bioessays* **19**, 469–479 (1997).
23. Mayer, B. J. SH3 domains: complexity in moderation. *J. Cell. Sci.* **114**, 1253–1263 (2001).
24. Thome, M. et al. Equine herpesvirus protein E10 induces membrane recruitment and phosphorylation of its cellular homologue, Bcl10. *J. Cell. Biol.* **152**, 1115–1122 (2001).
25. Hsi, E. D. et al. T cell activation induces rapid tyrosine phosphorylation of a limited number of cellular substrates. *J. Biol. Chem.* **264**, 10836–10842 (1989).
26. Chan, A. C., Iwashima, M., Turck, C. V. & Weiss, A. ZAP-70: a 70 kd protein-tyrosine kinase that associates with the TCR ζ chain. *Cell* **71**, 649–662 (1992).
27. Janes, P.W., Ley, S. C. & Magee, A. I. Aggregation of lipid rafts accompanies signaling via the T cell antigen receptor. *J. Cell Biol.* **147**, 447–461 (1999).
28. Leupin, O., Zaru, R., Laroche, T., Muller, S. & Valitutti, S. Exclusion of CD45 from the T-cell receptor signaling area in antigen-stimulated T lymphocytes. *Curr. Biol.* **10**, 277–280 (2000).
29. Legler, D. F., Doucey, M. A., Cerottini, J. C., Bron, C. & Luescher, I. F. Selective inhibition of CTL activation by a dipalmitoyl-phospholipid that prevents the recruitment of signaling molecules to lipid rafts. *FASEB J.* **15**, 1601–1603 (2001).
30. Harder, T. & Simons, K. Clusters of glycolipid and glycosylphosphatidylinositol-anchored proteins in lymphoid cells: accumulation of actin regulated by local tyrosine phosphorylation. *Eur. J. Immunol.* **29**, 556–562 (1999).
31. Doucey, M. A. et al. CTL activation is induced by cross-linking of TCR/MHC-peptide-CD8/p56<sup>lck</sup> adducts in rafts. *Eur. J. Immunol.* **31**, 1561–1570 (2001).
32. Ilangumaran, S., He, H. T. & Hoessli, D. C. Microdomains in lymphocyte signalling: beyond GPI-anchored proteins. *Immunol. Today* **21**, 2–7 (2000).
33. Bordier, C. Phase separation of integral membrane proteins in Triton X-114 solution. *J. Biol. Chem.* **265**, 1604–1607 (1991).
34. Schneider, P. et al. Characterization of two receptors for TRAIL. *FEBS Lett.* **416**, 329–334 (1997).
35. Kabouridis, P. S., Magee, A. I. & Ley, S. C. S-acylation of LCK protein tyrosine kinase is essential for its signalling function in T lymphocytes. *EMBO J.* **16**, 4983–4998 (1997).
36. Jain, J., Loh, C. & Rao, A. Transcriptional regulation of the IL-2 gene. *Curr. Opin. Immunol.* **7**, 333–342 (1995).
37. Su, B. et al. JNK is involved in signal integration during costimulation of T lymphocytes. *Cell* **77**, 727–736 (1994).
38. Bradley, J. R. & Pober, J. S. Tumor necrosis factor receptor-associated factors (TRAFs). *Oncogene* **20**, 6482–6491 (2001).
39. Devin, A. et al. The distinct roles of TRAF2 and RIP in IKK activation by TNF-R1: TRAF2 recruits IKK to TNF-R1 while RIP mediates IKK activation. *Immunity* **12**, 419–429 (2000).
40. Wang, C. et al. TAK1 is a ubiquitin-dependent kinase of MKK and IKK. *Nature* **412**, 346–351 (2001).
41. Thome, M. et al. Equine herpesvirus-2 E10 gene product, but not its cellular homologue, activates NF-κB transcription factor and c-Jun N-terminal kinase. *J. Biol. Chem.* **274**, 9962–9968 (1999).
42. Yoneda, T. et al. Regulatory mechanisms of TRAF2-mediated signal transduction by Bcl10, a MALT lymphoma-associated protein. *J. Biol. Chem.* **275**, 11114–11120 (2000).
43. Uren, A. G. et al. Identification of paracaspases and metacaspases: two ancient families of caspase-like proteins, one of which plays a key role in MALT lymphoma. *Mol. Cell* **6**, 961–967 (2000).
44. Dierlamm, J. et al. The apoptosis inhibitor gene API2 and a novel 18q gene, MLT, are recurrently rearranged in the t(1;18)(q21;q21)p6-associated with mucosa-associated lymphoid tissue lymphomas. *Blood* **93**, 3601–3609 (1999).
45. Akagi, T. et al. A novel gene, MALT1 at 18q21, is involved in t(1;18)(q21;q21) found in low-grade B-cell lymphoma of mucosa-associated lymphoid tissue. *Oncogene* **18**, 5785–5794 (1999).
46. Morgan, J. A. et al. Breakpoints of the t(1;18)(q21;q21) in mucosa-associated lymphoid tissue (MALT) lymphoma lie within or near the previously undescribed gene MALT1 in chromosome 18. *Cancer Res.* **59**, 6205–6213 (1999).
47. Lucas, P. C. et al. Bcl10 and MALT1, independent targets of chromosomal translocation in malt lymphoma, cooperate in a novel NF-κB signaling pathway. *J. Biol. Chem.* **276**, 19012–19019 (2001).
48. Ghaffari-Tabrizi, N. et al. Protein kinase Cθ, a selective upstream regulator of JNK/SAPK and IL-2 promoter activation in Jurkat T cells. *Eur. J. Immunol.* **29**, 132–142 (1999).
49. Alegre, M. L., Frauwirth, K. A. & Thompson, C. B. T-cell regulation by CD28 and CTLA-4. *Nature Rev. Immunol.* **1**, 220–228 (2001).
50. Penna, D. et al. Degradation of ZAP-70 after antigenic stimulation in human T lymphocytes: role of calpain proteolytic pathway. *J. Immunol.* **163**, 50–56 (1999).